Conduction-cooling of a high-temperature superconducting cable

Alberto Posada, Vasilios Manousiouthakis
Chemical & Biomolecular Engineering Department, University of California, Los Angeles, CA 90095, USA

Abstract

Current generation high-temperature-superconducting (HTS) power transmission cables use liquid nitrogen as a coolant that circulates along the cable. In this work, the use of axial conduction-cooling in attaining HTS temperatures in transmission lines is proposed. Liquid coolant use is envisioned only at periodic length intervals along the transmission lines, in combination with insulation and copper. The proposed concept is feasible due to the high thermal conductivity of pure copper at cryogenic temperatures. A basic design for the insulated cable is proposed and a detailed numerical simulation of heat transfer in such a cable is carried out for various case studies considering the superconducting materials MgB_2 and BSCCO-2223.

Keywords: Superconducting cables; High Tc superconductors; Copper; Conduction-cooling; Thermal conductivity.

1. Introduction

Several materials conduct electricity with zero resistance below a certain temperature, called critical temperature (T_c). Some examples of such superconducting materials are: $(Bi,Pb)_2Sr_2Ca_2Cu_3O_{10}$, also called BSCCO-2223 (T_c = 110 K), $YBa_2Cu_3O_7$ (T_c = 90 K) and MgB_2 (T_c = 39 K), [1]. Low cost cooling of superconducting devices below the transition temperature is an important goal for researchers who work in the field of energy applications in cryogenics. Power transmission lines made of low-temperature superconducting material are typically cooled, by convection, through circulation of liquid helium along the cable, [2-4]. The emergence of high–temperature-superconducting (HTS) material makes possible the use of liquid nitrogen as a coolant in transmission lines, thus reducing the operating cost of refrigeration [5-9]. Since in addition, HTS material has the advantage of high power density and zero environmental impact, power transmission lines using HTS cables are among the most promising applications of high-T_c superconductors.

The use of axial conduction-cooling in attaining HTS temperatures in transmission lines has been recently proposed by Manousiouthakis et al., [10]; liquid coolant use is envisioned at periodic length intervals along the transmission lines, in combination with insulation and copper, but no axial flow of liquid helium or nitrogen as coolant. The proposed concept is feasible due to the high thermal conductivity of pure copper at cryogenic temperatures [11]. A basic design for such a conduction-cooled high temperature superconducting power transmission cable is described and a detailed numerical simulation of heat transfer in such a cable is carried out using the partial differential equation solving software FEMLAB® version 2.3.

2. Description of the system

A schematic of a conduction-cooled high-temperature superconducting power transmission cable segment is presented in Fig. 1. It consists of a HTS wire that is surrounded by a layer of thermal insulator, a layer of copper and another layer of thermal insulator. The insulated wire segment is represented by a cylinder with radius R and length L. The HTS material is represented by the solid cylinder with radius r_1. The copper layer is represented by the hollow cylinder with internal radius r_2 and external radius r_3 (in white, see Fig. 1). The two remaining hollow cylinders, filled with gray color, separated by the copper layer, represent the two layers of thermal insulator. The cable ends are kept at low temperature (T_o) through the use of cryogenic refrigeration systems using liquid helium (T_o = 4.2 K), liquid hydrogen (T_o = 20.3 K) or liquid nitrogen (T_o = 77.4 K) while the ambient temperature is 300 K. The copper layer channels axially, towards the cable's cold ends, the heat that enters the cable radially through the outer insulation layer, instead of allowing it to move in the radial direction towards the cold superconductor.

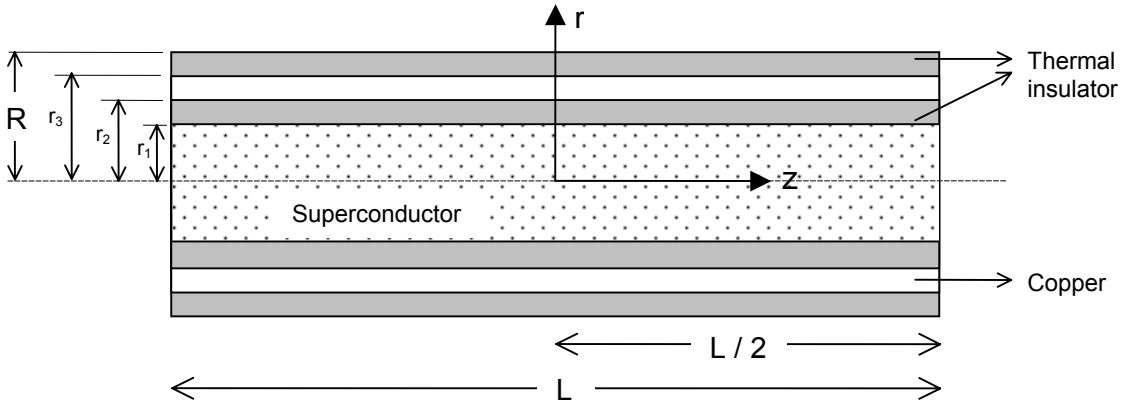

Fig 1. Schematic of a superconducting cable segment.

3. Thermal conductivity of materials

3.1. Copper

Eq. (1) gives the thermal conductivity k_c (W/m-K) for an average sample of oxygen-free copper, as a function of temperature, T (K), [11].

$$\log k_c = \frac{2.2154 - 0.88068 \cdot T^{0.5} + 0.29505 \cdot T - 0.048310 \cdot T^{1.5} + 0.003207 \cdot T^2}{1 - 0.47461 \cdot T^{0.5} + 0.13871 \cdot T - 0.020430 \cdot T^{1.5} + 0.001281 \cdot T^2} \quad (1)$$

The values calculated with Eq. (1) are plotted in Fig. 2. It can be noted that the thermal conductivity of copper at cryogenic temperatures reaches high values (over 2000 W/m-K).

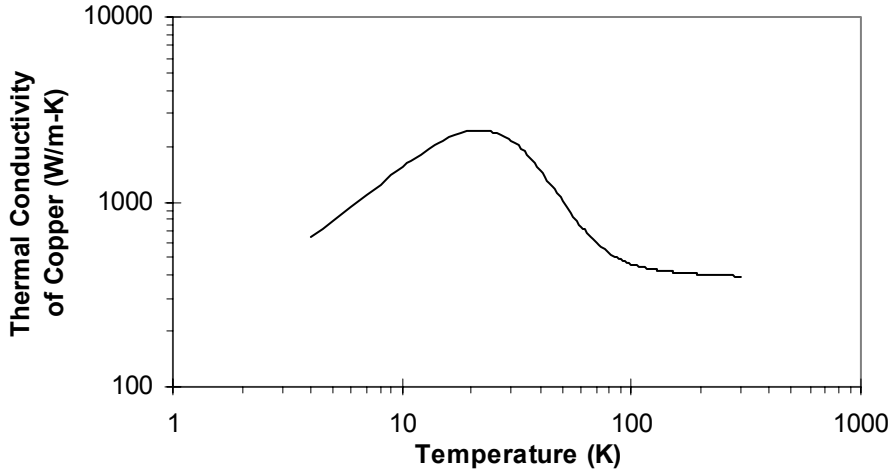

Fig 2. Thermal conductivity of copper, k_c, as calculated from Eq. (1).

3.2. Thermal insulator

A multilayer insulation is considered. It consists of alternating layers of a highly reflecting material, such as aluminum foil, and a low-conductivity spacer, such as fiberglass paper. The value of the thermal conductivity used for the calculations in this work, k_m = 3.7 x 10^{-5} W/m-K, corresponds to a multilayer insulation made with the materials mentioned above, with a layer density of 20 layer/cm [12].

3.3. Superconductor

Study cases in this work consider either MgB_2 (T_c = 39 K) or BSCCO-2223 (T_c = 110 K) as the HTS material employed in the superconducting layer. Data for thermal conductivity of MgB_2, k_{MgB2} (W/m-K), was obtained by Schneider et al., [13], at a wide range of temperatures, T (K). An approximate regression of this data for the range from 4 to 300 K is represented by Eq. (2). Schneider et al. found a positive slope of k_{MgB2} (T) in the whole investigated temperature range.

$$\begin{aligned}\log k_{MgB_2} = &-1.6158 - 3.8472\cdot\log T + 18.003\cdot(\log T)^2 - 21.307\cdot(\log T)^3 \\ &+ 12.111\cdot(\log T)^4 - 3.4362\cdot(\log T)^5 + 0.3905\cdot(\log T)^6\end{aligned} \tag{2}$$

Data for thermal conductivity of BSCCO-2223, k_{BSCCO} (W/m-K), was obtained by Castellazzi et al., [14], in the range from 20 to 220 K. An approximate regression of this data is represented by Eq. (3).

$$\begin{aligned}\log k_{BSCCO} = &-651.61 + 2308.7\cdot\log T - 3371.8\cdot(\log T)^2 + 2598.2\cdot(\log T)^3 \\ &- 1113.8\cdot(\log T)^4 + 251.85\cdot(\log T)^5 - 23.475\cdot(\log T)^6\end{aligned} \tag{3}$$

4. Heat transfer model

Considering steady state wire operation, as well as no angular dependence of the boundary conditions and of the thermal properties of all employed materials, heat transfer behavior, in each of the cable's regions, is captured by the differential equation:

$$0 = \frac{1}{r} \cdot \frac{\partial}{\partial r}\left(r \cdot k \cdot \frac{\partial T}{\partial r} \right) + \frac{\partial}{\partial z}\left(k \cdot \frac{\partial T}{\partial z} \right) \tag{4}$$

where k represents the thermal conductivity of the material and T is temperature. We consider the following boundary conditions:

$$T(z = \pm L/2) = T_o \qquad \forall r \in [0, R] \tag{5}$$

$$T(r = R) = T_e \qquad \forall z \in [-L/2,\ L/2] \tag{6}$$

where T_e is the ambient temperature (T_e = 300 K), and T_o is the low temperature imposed at the extremes of the cable, whose value depends on the coolant used (T_o = 4.2 K (for liquid helium), 20.3 K (liquid hydrogen) or 77.4 (liquid nitrogen)).

Due to the symmetry at z = 0, we can reduce the calculation domain work by considering only the solution for z ε [0, L/2], and a new boundary condition:

$$\frac{\partial T}{\partial z}(z = 0) = 0 \qquad \forall r \in [0, R] \tag{7}$$

Introducing the dimensionless variables:

$$r^* = \frac{r}{R} \qquad z^* = 2 \cdot \frac{z}{L} \qquad T^* = \frac{T - T_o}{T_e - T_o}$$

Eq. (4) can be written as:

$$0 = \frac{\partial}{\partial r^*}\left(r^* \cdot \frac{k}{R^2} \cdot \frac{\partial T^*}{\partial r^*} \right) + \frac{\partial}{\partial z^*}\left(r^* \cdot \frac{4 \cdot k}{L^2} \cdot \frac{\partial T^*}{\partial z^*} \right) \tag{8}$$

This equation is valid in each material as long as the proper value of thermal conductivity is used. Therefore we can write Eq. (8) for four different subdomains (i=1,..4), obtaining a system of four differential equations, as indicated below:

$$0 = \frac{\partial}{\partial r^*}\left(r^* \cdot \frac{k_i}{R^2} \cdot \frac{\partial T_i^*}{\partial r^*} \right) + \frac{\partial}{\partial z^*}\left(r^* \cdot \frac{4 \cdot k_i}{L^2} \cdot \frac{\partial T_i^*}{\partial z^*} \right) \qquad \text{for i=1,..4.} \tag{8-i}$$

where T_i^* is the dimensionless temperature in subdomain i and k_i is the thermal conductivity in subdomain i ($k_i = k_i(T_i^*)$). Thus Eq. (8-i) is valid for subdomain i. subdomain 1 ([0, $r_1^* = r_1/R$]) is the superconductor wire; subdomain 2 ([r_1^*, $r_2^* = r_2/R$]) is the inner insulation layer; subdomain 3 ([r_2^*, $r_3^* = r_3/R$]) is the copper layer; and subdomain 4 ([r_3^*, 1]) is the outer insulation layer. k_1; k_2 and k_4; k_3 are the thermal conductivities of superconductor; thermal insulator; copper respectively.

The resulting system of four second-order differential equations is solved for T_1^*, T_2^*, T_3^* and T_4^*, as functions of r^* and z^*, when combined with four boundary conditions in each subdomain (16 in total). In addition to the boundary conditions implied by (5), (6) and (7); and the one resulting from the radial symmetry at $r^* = 0$, we must consider the continuity of the temperature and the continuity of the radial heat flux at the interface between two subdomains.

5. Numerical solution

For a proper operation of a superconducting cable, it is necessary to maintain the temperature of the superconducting wire below its transition temperature. The temperature profile in the superconducting wire can be found by solving the system of Eqs. (8-i)(i=1,..4) for a particular cable configuration (specific values of r_i^* and L/R). Different cable configurations can be evaluated and those that result in temperatures below the superconductor's transition temperature can be used for superconducting power transmission. Three different cable configurations (Cases 1 to 3, see Table 1) employing MgB_2 superconducting wires and liquid helium refrigeration (T_o = 4.2 K) were considered here as examples to find numerical solutions and first demonstrate the feasibility of the proposed concept. Additional cable configurations employing BSCCO-2223 (Table 5) are included with the purpose of studying the effect of the end point refrigeration temperature as cooling with liquid nitrogen (T_o = 77.4 K) and liquid hydrogen (T_o = 20.3 K) is also evaluated.

The program FEMLAB® version 2.3 was used for the numerical calculation. With this software, the aforementioned PDE (Partial Differential Equation) problem is approximated using the Finite Element Method (FEM), [15]. FEMLAB® generates automatically a triangular mesh that covers the domain under consideration and takes into account the problem geometry. The approximate solution can be improved by increasing the number of elements in the mesh (refining the mesh), i.e. by dividing the elements into smaller elements.

6. Results and discussion

6.1. Case studies employing MgB_2

6.1.1. Case 1

Considering a cable with the specifications for Case 1 (see Table 1), the initial mesh constructed with the adaptive mesh generation tool of FEMLAB® contains 5,371 elements. Additional refinements of this mesh were done to improve the temperature profile approximation. An approximate numerical solution, obtained with a mesh of 231,082 elements, is presented in Fig. 3. This simulation indicates that the highest temperature in the

superconductor is attained at the interface with the inner insulation layer ($r^* = r_1^* = 0.8$) and in the middle of the axial length of the wire ($z^* = 0$, the furthest location from the cold ends), i.e. at (0, 0.8). Values for the temperature and the dimensionless temperature at this point, shown in Table 2, were calculated for increasingly refined meshes.

Table 1
Cable configuration for the three case studies employing superconducting material MgB_2 and liquid helium refrigeration (T_o = 4.2 K)

	Case 1	Case 2	Case 3
L/R	250	250	1000
r_1^*	0.80	0.20	0.20
r_2^*	0.85	0.30	0.30
r_3^*	0.90	0.40	0.40

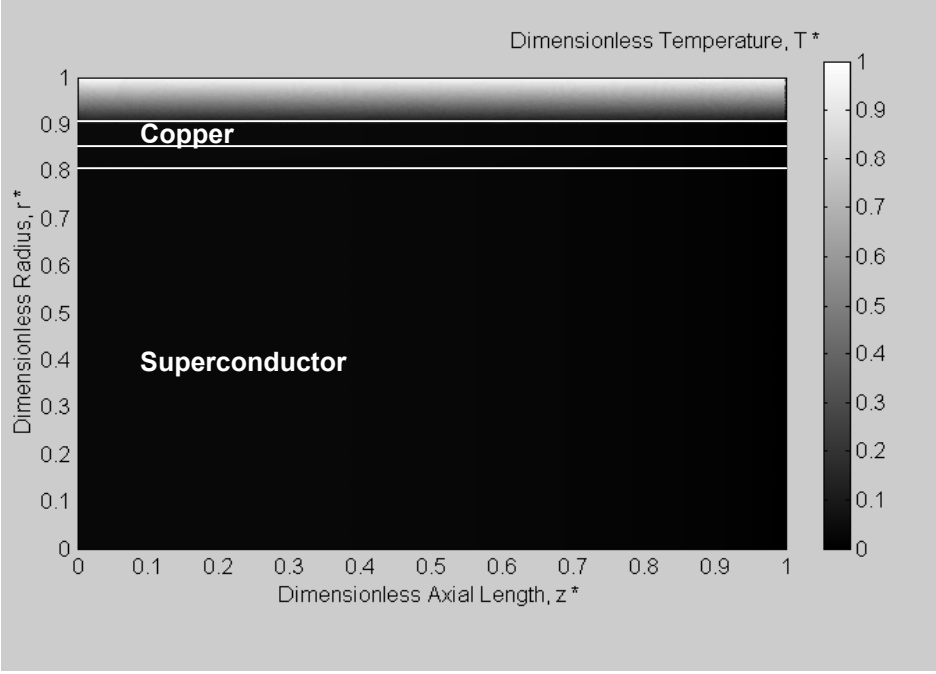

Fig. 3. Dimensionless temperature profile calculated with a mesh of 231,082 elements for Case 1.

Table 2
Calculated values for the highest temperature in the superconductor for a cable with the specifications of Case 1

Number of elements in the Mesh	T^* **(0, 0.8)** Case 1	T **(0, 0.8) (K)** Case 1
5,371	0.03686	15.1
15,641	0.03536	14.7
40,010	0.03502	14.6
97,054	0.03483	14.5
231,082	0.03470	14.5

6.1.2. Cases 2 and 3

The values calculated for the highest temperature in the superconductor, at the interface with the insulator at (0, 0.2), are shown in Tables 3 and 4, respectively.

Table 3
Calculated values for the highest temperature in the superconductor for a cable with the specifications of Case 2

Number of elements in the Mesh	T^* **(0, 0.2)** Case 2	T **(0, 0.2) (K)** Case 2
4,460	0.01098	7.4
12,831	0.01051	7.3
39,200	0.01033	7.2
116,838	0.01026	7.2

Table 4
Calculated values for the highest temperature in the superconductor for a cable with the specifications of Case 3

Number of elements in the Mesh	T^* **(0, 0.2)** Case 3	T **(0, 0.2) (K)** Case 3
4,511	0.08122	28.2
14,174	0.07959	27.7
48,270	0.07547	26.5
162,249	0.07320	25.9

For the three cases studied, the highest temperature calculated in the superconductor is below the transition temperature (T_c = 39 K) when a copper layer is incorporated in the cable insulation. Using the configurations described in these three cases, the temperature of the superconductor will be low enough to maintain the superconducting state.

The temperature of the superconductor calculated for case 1 is below 14.5 K (T^* = 0.03470, see Table 2). The temperature profile in Fig. 3 shows that the temperature decreases as the radial coordinate becomes smaller and also as we get closer to the cold end. If an insulated cable with radius, R, of 5 cm is considered, the length of the cable for Case 1 would be L = 12.5 m, and the radius of the superconductor wire, r_1 = 4 cm. A superconductor wire of MgB_2, with these dimensions, can therefore be kept below 14.5 K, which is a temperature low enough to assure the superconducting state of the wire.

The calculated axial heat flux is higher in the copper layer than in the other materials (close to 3 orders of magnitude higher when compared with the superconductor and 7 orders with respect to the thermal insulation layers), as expected due to copper's thermal conductivity. The copper layer is the preferred track for the heat, in such a way that most of the radial heat that passes through the outer insulation layer, coming from the environment, finds an easier way to continue along the copper towards the cold extremes, making this heat flux bigger, in general, as we move in this direction. Integration of the axial heat flux over the boundary of the cable at the cold extreme gives an approximation to the total heat flow transferred to the liquid helium at one extreme. For case 1 and L = 12.5 m, the value obtained is about 3.5 W, and over 95% of this heat comes from the copper layer.

An insulated cable with the same values for R and L, can be kept at even lower temperature if the radius of the superconductor wire is decreased and the thickness of the outer insulation layer is increased, as is done in Case 2 where the superconductor is kept below 7.2 K (see Table 3).

In order to study a longer cable, Case 3 considers a higher L/R ratio (L/R = 1000) than Case 2. In this case, an insulated cable with radius R =10 cm, length L = 100 m, and radius of the superconductor wire r_1 = 2 cm, can be kept below 25.9 K (see Table 4), which is a temperature lower than T_c for the employed HTS material MgB_2.

6.2. Case studies employing BSCCO-2223

Three different cable configurations are considered (see Table 5). They only differ in the value of r_3^*, i.e. the thickness of the copper and outer insulation layers. Cases 4-H to 6-H employ hydrogen coolant (T_o = 20.3 K) and Cases 4-He to 6-He employ helium coolant (T_o = 4.2 K). A L/R ratio of 2000 is employed for these six cases. Cases 4-N to 6-N employ nitrogen coolant (T_o = 77.4 K) and a L/R ratio of 500.

Heat transfer simulations for these cases also indicate that the highest temperature in the superconductor is attained at the interface with the inner insulation layer ($r^* = r_1^*$ = 0.1) and in the middle of the axial length of the wire (z^* = 0, the furthest location from the cold ends), i.e. at (0, 0.1). Calculated values for the temperature at this point are shown in Table 6 for all nine cases.

Table 5
Cable configuration for the nine case studies employing superconducting material BSCCO-2223

	Cases 4-H & 4-He	Cases 5-H & 5-He	Cases 6-H & 6-He	Case 4-N	Case 5-N	Case 6-N
L/R	2000	2000	2000	500	500	500
r_1^*	0.1	0.1	0.1	0.1	0.1	0.1
r_2^*	0.2	0.2	0.2	0.2	0.2	0.2
r_3^*	0.3	0.4	0.5	0.3	0.4	0.5

Table 6
Results of the numerical simulations carried out for the nine cases specified in Table 5

Case	T (0, 0.1)[a] (K)	Heat load[b] (W)	Elements in the mesh[c]
4-H	157.1	9	146,927
5-H	87.5	14	130,461
6-H	62.9	18	123,288
4-He	130.4	10	163,687
5-He	55.7	15	129,246
6-He	39.8	20	118,122
4-N	93.2	1.2	114,234
5-N	86.2	1.5	275,381
6-N	84.1	1.9	109,451

a: Temperature at (0, 0.1): the highest temperature in the superconductor.
b: Approximate total heat load removed by the coolant at the ends of a cable with radius R = 10 cm (both ends included)
c: Number of finite elements in the mesh generated by FEMLAB®

For an insulated cable with radius, R, of 10 cm and length, L, of 200 m (L/R = 2000), the approximate heat loads at the cable ends are given in the first six rows of Table 6 for those cases that use hydrogen or helium. The heat loads for the cases that use nitrogen are given for a cable with length, L, of 50 m (L/R = 500, R = 10 cm) in the same table. This heat is transferred from the environment to the cable and is pumped out of the cable by the coolant placed at the ends of the cable. More than 95 % of this heat is conducted through the copper layer towards the cold ends.

Given the critical temperature of BSCCO-2223, T_c = 110 K, for Cases 5-H, 6-H, 5-He, 6-He, 4-N, 5-N and 6-N, the temperature of the superconductor is low enough to maintain the superconducting state; but this doesn't happen for Cases 4-H and 4-He, where the temperature reaches values up to 157.1 and 130.4, respectively (see Table 6), exceeding the transition temperature.

Case 5-H employs a thicker copper layer and a thinner outer insulation layer, when compared to Case 4-H. This results in a lower maximum temperature in the superconductor, despite the higher radial heat flux entering the cable, due to the reduced thickness of the outer insulation layer. This reduced temperature is attributable to the increase in thickness of the copper layer, thus allowing increased axial heat flow towards the cable's cold ends. In this way most of the heat is prevented from reaching into the inner insulation and the superconducting wire, thus resulting in a lower superconductor temperature (below 87.5 K, see Table 6). Further increase in the thickness of the copper layer, as done in Case 6-H, gives an even lower temperature (below 62.9 K, see Table 6). On the other hand the heat load increases due to a thinner outer thermal insulation layer, reaching 18 W for Case 6-H (see Table 6).

Similar behavior is observed when we compare the three different cable configurations for the cases that employ helium coolant. Due to the lower normal boiling point of helium, the temperature attained in the superconductor, when helium is used, is lower than the one attained when hydrogen is used. Operation at lower temperature results in a higher heat load when helium is employed (20 W for Case 6-He, see Table 6), and therefore requires more refrigeration work. In addition, the lower efficiency of a refrigeration cycle that uses helium (the Carnot coefficient of performance is 5.1 times lower than the one for hydrogen) further increases refrigeration work for the case of helium.

Comparison of the different cable configurations for the cases that use nitrogen shows a similar effect of the copper layer's thickness variation on the maximum temperature in the superconductor and the heat load. In order to keep the superconductor's temperature below its transition value for the given cable radial configuration, a shorter cable has to be considered (here we used L/R = 500). This is due to the lower thermal conductivity of copper at the higher temperatures resulting from operation with nitrogen, and the smaller temperature range for which superconductivity is ensured.

If we consider four consecutive cable segments (50 m long each) employing nitrogen coolant every 50 m, the heat load for the resulting 200 m cable can be calculated as four times the one obtained for a 50 m cable, and shown in Table 6; for example, a 200 m cable with the configuration of Case 6-N has a heat load of 7.6 W (4 x 1.9W). By doing this for the three cases (4.8W for Case 4-N, 6W for Case 5-N) we find out that operation with nitrogen results in a lower heat load than hydrogen (and helium), due to a higher operation temperature for nitrogen. In addition, the higher efficiency of a refrigeration cycle that uses nitrogen (the Carnot coefficient of performance is 4.8 times higher than the one for hydrogen) results in a much lower refrigeration work for the case of nitrogen. Thus, from the viewpoint of refrigeration work required to keep the temperature of the superconductor below its transition value, nitrogen is preferable to hydrogen, and hydrogen is preferable to helium.

On the other hand, operation with nitrogen requires installation of a higher number of refrigeration units, located at shorter periodic length intervals, than hydrogen and helium; however each of these units is smaller in power requirement.

7. Conclusions

This work establishes the concept that a long HTS cable need not employ circulation of a cryogenic fluid coolant along the cable. The design of the superconducting cable with a copper layer incorporated in its thermal insulation, as described in this paper, achieves conduction-cooling of the superconductor wire to keep it below its transition temperature.

Several case studies are carried out using a variety of cable lengths, widths and insulation/copper layer thicknesses. The refrigeration work required for conduction-cooling of the BSCCO-2223 superconducting cable can be five (or even more) times lower when hydrogen coolant is employed instead of helium coolant. It can be reduced furthermore if nitrogen is employed instead of hydrogen, but refrigeration units are required at shorter periodic length intervals.

Acknowledgements

The authors gratefully acknowledge the financial support of the National Science Foundation under Grant CTS 0301931, and the US Department of State through a Fulbright Grant for Graduate Study.

References

[1] Nagamatsu J, Nakagawa N, Muranaka T, Zenitani Y, Akimitsu J. Superconductivity at 39 K in magnesium diboride. Nature 2001;410:63-4.
[2] Borgner G. Cryopower transmission studies in Europe. Cryogenics 1975;15:79-87.
[3] Belanger BC. Superconducting power transmission programme in the USA. Cryogenics 1975;15:88-90.
[4] Horigome T. The present state of R & D for superconducting transmission in Japan. Cryogenics 1975;15:91-4.
[5] Wesche R, Anghel B, Jakob B, Pasztor G, Schindler R, Vecsey G. Design of superconducting power cables. Cryogenics 1999;39:767-75.
[6] Furuse M, Fuchino S, Higuchi N. Counter flow cooling characteristics with liquid nitrogen for superconducting power cables. Cryogenics 2002;42:405-9.
[7] Masur L, Parker D, Tanner M, Podtburg E, Buczek D, Scudiere J, Caracino P, Spreafico S, Corsaro P, Nassi M. Long length manufacturing of high performance BSCCO-2223 tape for the Detroit Edison power cable project. IEEE Trans. Appl. Supercond. 2001;11(1):3256-60.
[8] Kellers J, Masur LJ. Reliable commercial HTS wire for power applications. Physica C 2002;372-376:1040-5.
[9] Van Sciver SW. Cryogenic systems for superconducting devices. Physica C 2001;354:129-35.
[10] Manousiouthakis V, Kim YI, Posada A. Conduction cooling of a superconducting cable. World Patent WO2005020245, 2005.
[11] Marquardt ED, Le JP, Radebaugh R. Cryogenic material properties database. Proceedings of the 11th International Cryocooler Conference, June 2000, Keyston, CO, USA.
[12] Barron RF. Cryogenic systems. 2nd ed. New York: Oxford University Press, 1985.

[13] Schneider M, Lipp D, Gladun A, Zahn P, Handstein A, Fuchs G, Drechsler S, Richter M, Müller K, Rosner H. Heat and charge transport properties of MgB_2. Physica C 2001;363:6-12.
[14] Castellazzi S, Cimberle MR, Ferdeghini C, Giannini E, Grasso G, Marre D, Putti M, Siri AS. Thermal conductivity of a BSCCO(2223) c-oriented tape: a discussion on the origin of the peak. Physica C 1997;273:314-22.
[15] COMSOL AB. FEMLAB® Reference Manual. 2nd printing. Stockholm: COMSOL AB, 2001.